DESIGN AND TEST OF TRACTION COMBINED MACHINE FOR SUBSOILING AND LAND PREPARATION
/
牵引式深松整地联合作业机设计与试验

Jingyu LI, Sihao ZHANG, Pengfei ZHANG, Wenjun WANG *)
School of Agricultural Engineering and Food Science, Shandong University of Technology, Zibo/China;
Tel: +86-15550326189; E-mail: wjwang2016@163.com
Corresponding author: Wenjun Wang
DOI: https://doi.org/10.35633/inmateh-68-28

Keywords: *conservation tillage, subsoiler, soil crushing, stalks mulching, variable fertilization, hydraulic control system*

ABSTRACT
In order to solve the problems of crop residue clogging, poor soil crushing and low operation efficiency under the stalks mulching condition, the traction combined machine for subsoiling and land preparation was designed. The optimization test was carried out to optimize the stalk cutting device and the soil crushing device under stalk mulching condition. The optimization test used a randomized complete block design, consisting of 10 treatments, in a 5 × 2 factorial arrangement. Each treatment included the combination of coulter types (8W, 13W, 18W, 25W and NW) and soil crushing roller types (with blade angle and without blade angle). The results showed that the combination of the fluted coulters with 8 waves and the soil crushing roller with blade angle was optimal. Finally, the verification test of the whole machine was carried out to evaluate the performance, and the results showed that the average value of subsoiling depth was 35.8 cm, the stability coefficient of subsoiling depth was 93.9% and the soil crushing rate was 53.7%. This research provides an important reference for the structure design of the large multi-functional combined machine for conservation tillage.

摘要
为解决秸秆覆盖条件下深松作业缠绕堵塞严重，以及作业效率低等问题，研制了牵引式深松整地机，包括新型切茬松土装置、仿形碎土装置、液压控制系统和变施肥控制系统。通过田间优化试验探究全量秸秆覆盖条件下新型切茬松土装置和仿形碎土装置对整机性能的影响，试验因素包括耕刀类型（8W, 13W, 18W, 25W and NW）和碎土轮类型（有叶片倾角和无叶片倾角两种），优化试验结果表明，8 波纹的犁刀与带叶片角的碎土辊组合使用效果最佳。最后进行了整机田间验证试验，结果表明：平均深松深度为35.8 cm，深松稳定系数为93.9%，土壤破碎率为53.7%，该研究为保护性耕作条件下的大型深松整地联合作业机设计提供参考。

INTRODUCTION
In the past 30 years, the long-term use of small-scale mechanical rotary tillage instead of deep plowing has caused soil compaction, severe wind and water erosion, poor drought and waterlogging resistance, difficulty in deep rooting of crops, and frequently crop lodging in autumn, seriously endangering food production (*Daraghmeh et al., 2019; Qi et al., 2020; Qu et al., 2021*). Conservation tillage has been described as one of the key solutions to these problems. Research results in recent years have shown that the use of conservation tillage mode, including stalk returning, subsoiling and no-tillage planting, is an effective method to improve the ecological environment, increase soil water storage capacity and fertility, and maintain sustainable agricultural development (*Wang et al., 2016; Issaka et al., 2019; Mondal et al., 2019*). Subsoiling refers to the soil loosening operation that exceeds the normal plow depth, destroying the hard plough pan, increasing water storage capacity and improving the growth environment of crops (*Guo et al., 2021*). Especially for deep root crops, subsoiling is an important technology to increase production (*Qi et al., 2018*).

The subsoiler creates a "virtual and solid coexistence" tillage layer structure that is different from traditional plowing. The subsoiling breaks the plough pan and only loosens the soil without turning it, establishing a suitable growing environment and improving the ability to resist drought and soil erosion. Practice has proved that subsoiling technology has strong pertinence and obvious effect on mitigating spring drought and soil erosion during the rainy season in northern China (*Zhang et al., 2018*).

With the application and popularization of high-power tractors, agricultural machinery has generally developed in the direction of large-scale and combined operations, which are characterized by large subsoiling depth, high work efficiency, and good work quality (*Celik et al., 2012; Prathuang et al., 2018; Jiang et al.,*

2020). Therefore, it is necessary to develop the combined machine for subsoiling and land preparation to overcome the serious soil compaction caused by the repeated operation of small-scale machines.

In addition, the traditional subsoiling machine works well in the cropland without mulch, but the operating effect is significantly reduced in the cropland with mulch (*Jia et al., 2017; Wang et al., 2021*). Under the stalk mulching condition, the phenomenon of crop residue clogging will occur during subsoiling operation, especially when the straw cover ratio reaches more than 90%, the working resistance caused by straw blocking increases by more than 20% (*He et al., 2018*). In addition, the subsoiler will squeeze the upper soil to uplift the surface soil during subsoiling operation, forming a large number of soil blocks. The large gaps between these soil blocks will cause the moisture to disperse quickly (*Feng et al., 2018*). Therefore, it is necessary to develop a subsoiling machine that can adapt to the cropland mulched stalk and stubble, and solve the problems of crop residue clogging and poor soil crushing under the condition of stalk mulching.

In order to solve the above problems, we designed the traction combined machine for subsoiling and land preparation, which can perform several operations in a single pass, reduce the number of passes of the agricultural machine on the cropland and improve work efficiency. The field optimization test was carried out to optimize the parameters of the key components and evaluate the machine performance under stalk mulching condition.

MATERIALS AND METHODS

General design of traction combined machine for subsoiling and land preparation

The traction combined machine for subsoiling and land preparation is mainly composed of four functional modules: stalk cutting and topsoil loosening, subsoiling, variable fertilization and land preparation. The four modules are reasonably configured and work independently to achieve the combined operation. The whole structure of the machine is shown in Fig. 1.

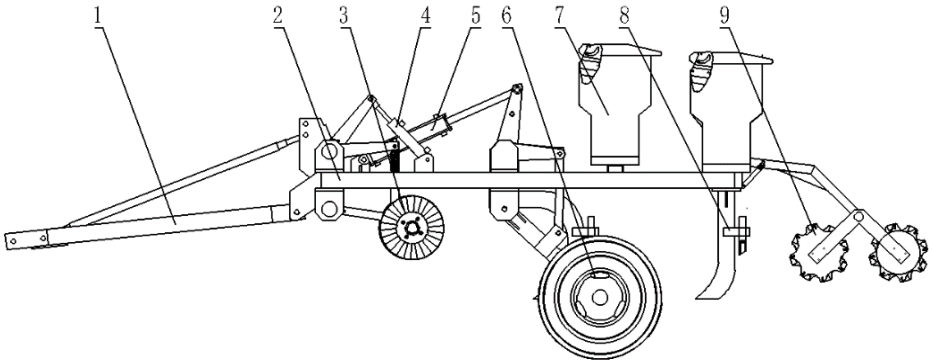

Fig. 1 - Whole structure of the machine

1-Traction frame; 2-Main frame;3-Stalk cutting device; 4-Stalk cutting device cylinder; 5-Land wheel cylinder; 6-Land wheel; 7-Fertilizer box; 8-Subsoiler; 9-Soil crushing device

The main frame was composed of three beams: front beam, middle beam and rear beam. Seven sets of stalk cutting devices were hinged on the front beam. The subsoilers were fixed to the middle beam and the rear beam. The land wheels were hinged on the middle beam to control the lifting of the whole machine. The soil crushing devices were hinged on the rear beam. The stalk cutting devices were controlled by stalk cutting device cylinder, and the land wheels were controlled by land wheel cylinder. The main technical parameters of the whole machine are shown in Table 1.

Table 1

Main technical parameters of the machine

Parameter	Value
Overall dimension, L×W×H (mm×mm×mm)	5800×4640×1500
Working rows	7
Row spacing (mm)	600-700
Power requirements (kW)	88.2-132.3
Working speed (km/h)	3-5
Maximum subsoiling depth (mm)	40
Mass (kg)	1300

Design of the hydraulic control system

In order to reduce the work intensity of the operator, the hydraulic control system was designed. The working principle of the hydraulic control system is shown in Fig. 2. The hydraulic control system was divided into two independent parts: the hydraulic control system of land wheels (Fig. 2A) and the hydraulic control system of stalk cutting devices (Fig. 2B). The hydraulic oil of the entire system came from the tractor.

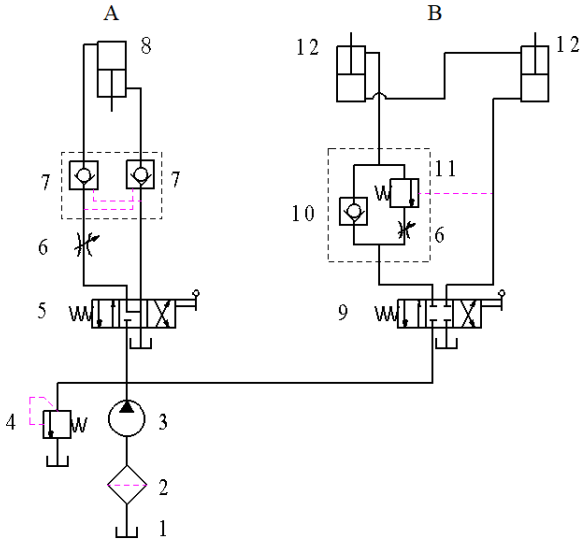

Fig. 2 - Working principle of the hydraulic control system.

1-Hydraulic fluid chamber; 2-Filter; 3-Oil pump; 4-Overflow valve; 5-Hand-operated direction valve with Y-type median function; 6-Throttle valve; 7-Pilot operated check valve; 8-Land wheel cylinder; 9-Hand-operated direction valve with O-type median function; 10-Check valve; 11-Sequence valve; 12-Stalk cutting device cylinder

(1) Whole structure design

The hydraulic control system of land wheels is shown in Fig. 3a. The switching between work state and transport state of the whole machine is realized by the land wheel cylinder. The switching between transport state and working state of the whole machine should meet two conditions: the height of the subsoiler tip from the cropland is more than 300 mm under transport state and the subsoiler tip is 400 mm below the cropland at the maximum working depth. The switching process of the two states is shown in Fig.3. The solid line outline in Fig. 3b indicates the transport state of the whole machine. At this time, the height of the machine from the cropland is maximum and the land wheel cylinder is at the maximum stroke. The dotted line outline in Fig. 3b indicates the maximum working depth of the machine.

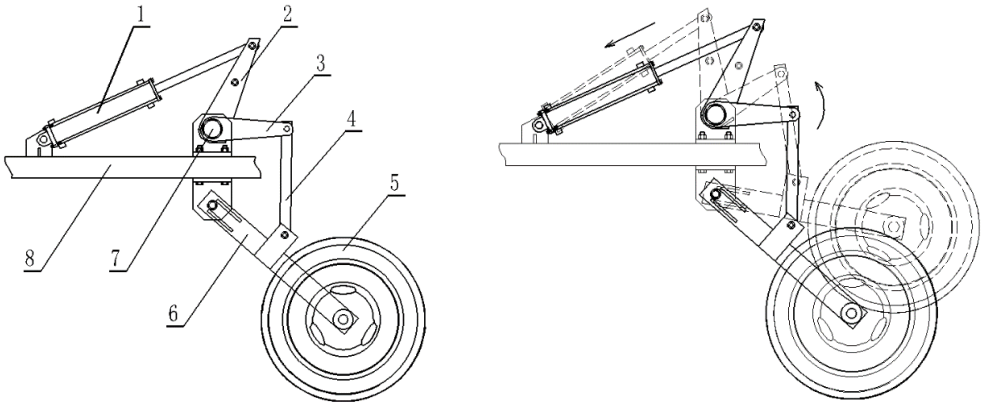

a. Structure diagram *b. State switching process*

Fig. 3 - Structure of the hydraulic control system of land wheels

1-Land wheel cylinder; 2-Main swing arm; 3-Lifting swing arm; 4-Linkage; 5-Land wheel; 6-Wheel frame; 7-Rotating shaft; 8-Frame of whole machine

In order to adapt to the no-till cropland with a large amount of straw mulch, the stalk cutting device with a symmetrical double-coulter was designed, as shown in Fig. 4a. The device can cut the long stalks and weeds to avoid the tangling and clogging of subsoiler, and can also play the role of loosening the topsoil.

The lifting of the stalk cutting devices is controlled by the stalk cutting device cylinder, as shown in Fig. 4b. The device can float up and down around the rotating shaft during the work process. The spring can maintain the stalk cutting and topsoil loosening pressure of the coulter. When the coulter encounters hard stalk or soil, the upward pressure acted on the coulter increases, and the stalk cutting devices float upward. At this time, the pressure of the spring gradually increases until the hard stalk or soil is chopped. So, the stalk cutting devices float with the undulation of the cropland surface to prevents damage caused by excessive stress.

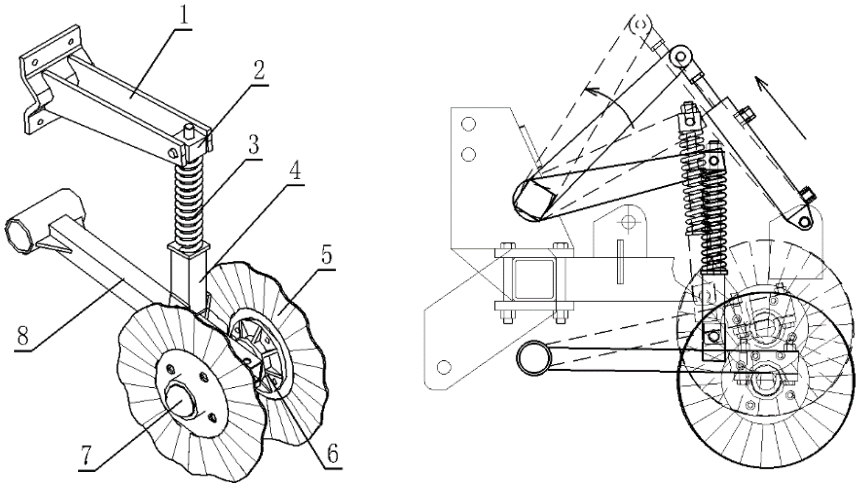

a. Structure diagram *b. working process*

Fig. 4 - Structure of the hydraulic control system of stalk cutting devices

1-Upper swing arm; 2-Pressure rod; 3-Spring; 4-Pressure rod tube; 5-Coulter; 6-Bearing seat; 7-Dust cap; 8-Lower swing arm

(2) Hydraulic actuators design

The working pressure of the hydraulic transmission system could be selected according to the maximum load in the load diagram of the actuator, or according to the type of the machine. The working pressure of the hydraulic system in general agricultural machine was 10-16 MPa, so the maximum pressure selected in this research was 16 MPa.

The hydraulic actuators included the land wheel cylinder and the stalk cutting device cylinder, so it was necessary to calculate the body diameter and rod diameter of two types of hydraulic cylinders.

The maximum mass of the whole machine that the land wheel cylinder needs to overcome was 1300 kg, and the cylinder load was the largest when it reached the maximum stroke, which was about 3 times the weight of the whole machine, that was, F=39000 N. Then the working area of the land wheel cylinder was:

$$A = \frac{F}{p} = \frac{\pi(D^2 - d^2)}{4} \quad (1)$$

where: D is body diameter, m; F is load, N; p is system pressure, Pa; d is rod diameter, m, d = 0.4D.

Substitute p and F into the formula (1) to get D=70 mm. According to the standard specification of hydraulic cylinder, the selected body diameter was D=63 mm, so the selected rod diameter was d =25 mm for the land wheel cylinder.

For the stalk cutting device cylinder, the load was the maximum pressure of coulters. The pressure of a coulter required 1946 N (*Wang et al., 2012*), which was the basis for calculating the pressure of hydraulic cylinders. In the paper, there were seven sets of double coulters and two cylinders in the whole machine, so the load of each cylinder was 13622 N respectively. Similarly, the formula (1) could be used to determine that the body diameter was 40 mm and the rod diameter was 16 mm for the stalk cutting device cylinder.

For the land wheel cylinder and the stalk cutting device cylinder, the rod strokes should not exceed 500 mm and 300 mm respectively, and the time required for lowering or raising was 20 s. The flow rate could be calculated by the following formula.

$$Q = \frac{\pi}{4} \cdot D^2 \cdot \frac{S}{t} \quad (2)$$

where, Q is the maximum flow rate of hydraulic cylinder, m^3/s; S is the stroke of hydraulic cylinder, m;

t is the time required for lowering or raising, s.

Substituting D, S, and t into the formula (2), it was obtained that the flow rate was 11.8 L/min for the land wheel cylinder and 4.5 L/min for the stalk cutting device cylinder.

Design of the variable fertilization control system

The variable fertilization software run on PIC18F2682, the single chip microcomputer (micro control unit) collected the speed sensor signal to calculate the forward speed of the machine, and controlled the speed of stepper motor according to the fertilization formula to implement variable fertilization. The working principle of variable fertilization control system is shown in Fig. 5.

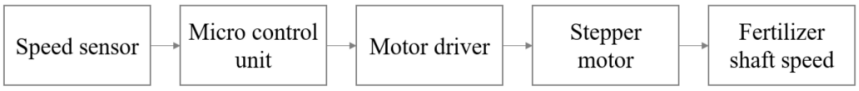

Fig. 5 - Schematic of the variable fertilization control system

The forward speed and the speed count-pulse meet the following formula:

$$v = \frac{I}{N} \cdot \pi D \times 3.6 \quad (3)$$

where, v is the forward speed of the machine, km/h; I is the number of speed pulses per unit time, s^{-1}; N is the number of magnets on the wheel hub used for counting; D is the diameter of the wheel used for counting, m.

The fertilizing amount should meet the following formula:

$$q = \frac{1}{6} vBQ \times 10^{-4} \quad (4)$$

where, q is the fertilizing amount per unit time of each fertilizer apparatus, kg/min; B is the row spacing of fertilizing operation, B=0.65 m; Q is the fertilizing amount per hectare, kg/hm^2.

The fertilizing amount per unit time of each fertilizer apparatus q and the rotation speed of the fertilizing shaft n meet the following formula:

$$q = kn + b \quad (5)$$

where, n is the rotation speed of the fertilizing shaft, r/min; k and b are the constant coefficient, k=0.032, b=0.1935.

Substituting formula (5) into formula (4), we can get:

$$n = (\frac{1}{6} vBQ \times 10^{-4} - b)/k \quad (6)$$

According to formula (6), the rotation speed of the fertilizing shaft can be changed automatically with the forward speed just by inputting Q value into the system before operation. The system can input different Q values according to the requirements of different regions or plots for fertilizer.

Design of the soil crushing device

The soil crushing device is arranged behind the subsoiler to finely break the surface soil after subsoiling. The soil crushing device designed is shown in Fig. 6a, including two soil crushing rollers, which can achieve profiling on the cropland surface around the rotation points 1 and 2.

The surface of the soil crushing roller is evenly distributed with blades, and each blade rolls into the soil gradually with the rolling of the roller. According to the twisting direction of blades, the soil crushing roller can be divided into the roller with left-rotation blades (Fig. 6b) and the roller with right-rotation blades (Fig. 6c). Two type rollers are combined into the soil crushing device, which can further crush and suppress the surface soil to form a flat seed bed. With reference to rod-type spiral soil crushing roller, the blade angle of the soil crushing roller is 15°.

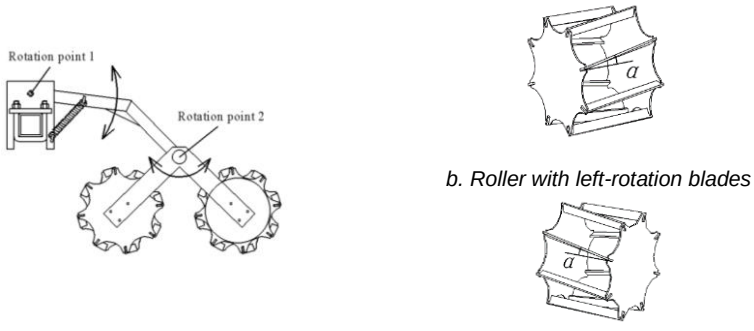

a. Profiling principle *b. Roller with left-rotation blades* *c. Roller with right-rotation blades*

Fig. 6 - Structure of the soil crushing device. Note: α is the blade angle of the soil crushing roller.

Test plot

The field test was conducted in the test field at Shandong University of Technology, Zibo, China. The last crop of the test plot was corn, the stubbles and stalks were left on the cropland after harvesting in autumn. The field test consisted of two parts: optimization test and verification test.

Test scheme and method

(1) Optimization test

The traction came from the Deere 1404 tractor, and the working speed was about 0.9 m/s in the optimization test. The different coulters and different soil crushing rollers were selected to test. The coulters had five levels: four fluted coulters (with 8, 13, 18, 25 waves) and one flat coulter (without wave), which were named as 8W, 13W, 18W, 25W and NW, respectively. The soil crushing rollers had two levels: with blade angle (α=15°) and without blade angle (α=0°). So there were 10 treatments in the optimization test. The test indicators were the stalk cutting rate and soil crushing rate. The test area was 100 m long and 50 m wide. For each treatment, one coulter and one soil crushing roller were selected to work on the test plot.

Measurement of stalk cutting rate: All the stalks touched by the coulter were collected and counted. The stalk cutting rate was calculated according to the following formula.

$$T = \frac{a}{a+b} \times 100\% \tag{7}$$

where, T is the stalk cutting rate, %; a is the number of stalks cut; b is the number of stalks uncut.

Measurement of soil crushing rate: Randomly take 10 measuring points with an area of 0.5 m×0.5 m to measure the quality of the soil block with the longest side less than 4 cm and the total quality of all soil block, respectively. The soil crushing rate was calculated according to the following formula, and the average value was taken as the final result.

$$C = \frac{G_a}{G} \times 100\% \tag{8}$$

where, C is the soil crushing rate, %; G_a is the quality of the soil block with the longest side less than 4 cm, kg; G is the total quality of all soil block, kg.

(2) Verification test

The purpose was to verify the operating performance of the whole machine under optimal parameter combination conditions, including subsoiling performance, soil crushing performance and fertilizing performance. The corresponding test indicators were the subsoiling depth and the stability coefficient of subsoiling depth, the soil crushing rate, the variation coefficient of fertilizing amount in each row and the variation coefficient of total fertilizing amount. The set theoretical subsoiling depth was 35 cm, and the presupposed fertilizing amount was 150, 400, 800 kg/hm^2 respectively. The whole machine worked back and forth once in the test plot with 100 m long.

Subsoiling performance: In the measurement area, 5 points were randomly selected for each row to measure the subsoiling depth. The stability coefficient of subsoiling depth ε was calculated by the following formula.

$$\varepsilon = 1 - \sqrt{\frac{\sum(h_i - \bar{h})^2}{n-1}} / \bar{h} \times 100\% \tag{9}$$

where, ε is the stability coefficient of subsoiling depth, %; h_i is the subsoiling depth at the i-th point, mm; $\bar{h}$ is the average value of subsoiling depth, mm; n is the number of measured points.

Soil crushing performance: Randomly take 10 measuring points with an area of 0.5 m×0.5 m for each row to measure. The measurement method is the same as that described in the optimization test. The soil crushing rate was calculated according to the formula (8) and the average value was taken as the final result.

Fertilizing performance: The fertilizing performance test was carried out when the machine was parked. All 7 rows were tested, and the measurement time was 30 s each time, repeated 5 times. The variation coefficient of fertilizing amount in each row ζ_r and the variation coefficient of total fertilizing amount ζ_t were calculated by the following formulas:

$$\zeta_r = \sqrt{\frac{\sum(Q_i - \overline{Q_r})^2}{k-1}} / \overline{Q_r} \times 100\% \tag{10}$$

$$\zeta_t = \sqrt{\frac{\sum(Q_j - \overline{Q_t})^2}{m-1}} / \overline{Q_t} \times 100\% \quad (11)$$

where, ζ_r is the variation coefficient of fertilizing amount in each row, %; Q_i is the fertilizing amount for the i-th row, g; $\overline{Q_r}$ is the average value of the fertilizing amount of the each row, g; k is the number of measurements; ζ_t is the variation coefficient of total fertilizing amount, %; Q_j is the value of total fertilizing amount for the j-th time, g; $\overline{Q_t}$ is the average value of total fertilizing amount of the each time, g; m is the number of rows.

The field test site is shown in Fig. 7.

a. Physical prototype *b. Operation process*

Fig. 7 - Field test site

RESULTS AND DISCUSSION

Optimization test

The data of optimization test were processed and analyzed using SPSS version 19.0 statistical software (SPSS Inc., Chicago). The analysis of variance (ANOVA) of each variable with their means, level and F test results are shown in Table 2.

The effect of coulter types on the stalk cutting rate was not significant (P≥0.05) (Table 2). The results showed that the stalk cutting rate was 97.7%-99.2%, which means the stalk cutting device with double-row coulter could effectively cut stalks covering the cropland, regardless of the coulter types. The reason was that the hydraulic control system gave a large downforce during operation, which is enough to cut the straw by different types of coulters.

Table 2

Statistical analysis of the different factors and their interactions

Factors	Variables	
	Stalk cutting rate (%)	Soil crushing rate (%)
Coulter types (F1)		
NW	99.2a	33.7e
8W	98.4a	52.5a
13W	97.7a	47.0b
18W	98.1a	43.3c
25W	97.9a	40.8d
Soil crushing roller types (F2)		
With blade angle	/	46.7a
Without blade angle	/	40.2b
F-test		
F1	0.35ns	614.23**
F2	/	54.31**
F1×F2	/	3.28*

*Note: 8W, 13W, 18W, 25W and NW respectively represent four fluted coulters (with 8, 13, 18, 25 waves) and one flat coulter (without wave). Means followed by the same letter in the column do not differ significantly by LSD's test (p≥ 0.05). **significant at 1% probability (p < 0.01). *significant at 5% probability (p < 0.05). ns: non-significant (p≥ 0.05). F-test is any statistical test in which the test statistic has an F-distribution under the null hypothesis.*

The effects of coulter types and soil crushing roller types on soil crushing rate were both very significant ($P<0.01$), and there was a significant interaction between the two factors ($P<0.05$) (Table 2).

The soil crushing rate of NF was the smallest (33.7%) in all treatment. The soil crushing rate of 8W, 13W, 18W and 25W were 55.8%, 39.5%, 28.5%, 21.1% higher than that of NF respectively (Table 2, Fig. 8). With the increase of the number of waves for the fluted coulter, the soil crushing rate gradually decreased. The reason was that the surface soil was loosened by the double-row fluted coulter before the subsoiling operation, it was not easy to form large soil blocks on the surface during subsoiling operation. The smaller the number of waves, the larger the range of soil loosening, which would cause more disturbance of the surface soil and the less likely to form large soil blocks. For the NF coulter, its main function was to cut the stalk, and the soil loosening performance was poor, so it was easier to form large soil blocks than fluted coulters. Wang et al. reported that a different working width resulted in a different soil disturbance width, and a narrower tool created less soil disturbance normally (*Wang et al., 2018*). Zeng et al. also got the same conclusion (*Zeng et al., 2018*).

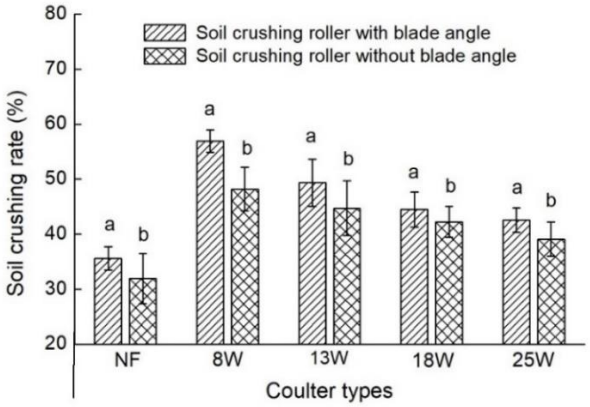

Fig. 8 - Effect of coulter types and soil crushing roller types on soil crushing rate

Note: The same letters over bars indicate groups which were not significantly different (P≥0.05)

The soil crushing roller with blade angle had a better soil crushing effect, and its soil crushing rate was 16.2% higher than that without blade angle (Table 2, Fig. 8). The reason was that the blade angle could ensure the blades gradually entered the soil, and there be sufficient shear force to cut large soil blocks during this process. Compared with the soil crushing roller without blade angle, the combined action of the soil crushing rollers with left-rotation blades and right-rotation blades made the leakage area less. In addition, the special profiling structure could make the double soil crushing roller to move close to the cropland surface, making the soil more finely broken.

For subsoiling operations, a higher soil crushing rate could effectively reduce soil moisture loss (*Borek et al., 2018*), so the combination of the fluted coulters with 8 waves (8W) and the soil crushing roller with blade angle was optimal.

Verification test

The test results of subsoiling performance obtained are shown in Table 3. It can be seen that the average value of subsoiling depth was 35.8 cm, slightly larger than the theoretical subsoiling depth of 35 cm, and the stability coefficient of subsoiling depth was 93.9%, which met the design requirements of the China National Standard No. GB/T 24675.2-2009 ($\varepsilon \geq 85\%$).

Test results of subsoiling performance **Table 3**

Row	Measuring point (cm)					Row average value (cm)	Total average value (cm)	Stability coefficient ε (%)
	1	2	3	4	5			
Row 1	41.0	35.2	36.1	40.1	35.2	37.5		
Row 2	37.5	40	33.2	37.9	39.5	37.6		
Row 3	38.3	37.2	36.7	34.5	30.6	35.5		
Row 4	32.3	36.6	33.4	31.4	33.2	33.4	35.8	93.9
Row 5	38.2	37.3	39.5	37.9	40.5	38.7		
Row 6	34.4	33.7	35.2	30.5	33.9	33.5		
Row 7	35.2	31.6	34.7	36.4	32.4	34.1		

The test results of soil crushing performance obtained are shown in Table 4. It can be seen that the soil crushing rate met the design requirements of the China National Standard No. GB/T 24675.2-2009 (C≥30%).

Table 4

Test results of soil crushing performance

Row	Row 1	Row 2	Row 3	Row 4	Row 5	Row 6	Row 7	Average
Soil crushing rate *C* (%)	54.3	43.4	60.7	58.9	62.4	51.2	45.2	53.7

The test results of fertilizing performance obtained are shown in Table 5. It can be seen that the fertilizing amount can be adjusted in the range of 150-800 kg/hm^2. With the increase of the fertilizing amount, the variation coefficient of fertilizing amount in each row increases, while the variation coefficient of total fertilizing amount decreases. Both test indicators met the design requirements of the China Agricultural Industry Standard No. NY/T1003-2006 (ζ_r≤13%, ζ_t≤7.8%).

Table 5

Test results of fertilizing performance

Presupposed value (kg/hm^2)	800	400	150
$\overline{Q_r}$ (g)	2195.2	1192.5	404.8
ζ_r (%)	4.1	7.6	11.2
$\overline{Q_t}$ (g)	13171.1	7155.3	2429
ζ_t (%)	3.3	3.2	1.5

CONCLUSIONS

The traction combined machine for subsoiling and land preparation was designed, including the new stalk cutting device with double-row coulter, the soil crushing device with profiling structure, the hydraulic control system and the variable fertilization control system. The machine can complete the functions of stalk cutting and topsoil loosening, subsoiling, variable fertilization and land preparation in one operation, solving the problems of crop residue clogging, poor soil crushing and low operation efficiency in the cropland covering stalks.

The field optimization test was carried out to evaluate the effects of coulter types and soil crushing roller types on the machine performance. The results showed that the combination of the fluted coulters with 8 waves (8W) and the soil crushing roller with blade angle was optimal.

The results of field verification test showed that all performances met the design requirements of the relevant standards. This research provides an important reference for the structure design of stalk cutting device and soil crushing device for conservation tillage. The large multi-functional combined machine is the developing direction of agricultural equipment in the future.

ACKNOWLEDGEMENT

This work was supported by the National Natural Science Foundation of China (Grant No. 52005307).

REFERENCES

[1] Borek L., Bogdal A., Ostrowski K., (2018), The effect of subsoiling on changes of compaction and water permeability of silt loam, *Rocznik Ochrona Srodowiska*, vol.20, pp.538-557.

[2] Celik A., Raper R.L., (2012), Design and evaluation of ground-driven rotary subsoilers, *Soil and Tillage Research*, vol.124, pp.203-210.

[3] Daraghmeh O.A., Petersen C.T., Munkholm L.J., Znova L., Obour P.B., Nielsen S.K., Green O., (2019), Impact of tillage intensity on clay loam soil structure, *Soil Use and Management*, vol.35, no.3, pp.388-399.

[4] Feng X.M., Hao Y.B., Latifmanesh H., Lal R., Cao T.H., Guo J.R., Deng A.X., Song Z.W., Zhang W.J., (2018), Effects of subsoiling tillage on soil properties, maize root distribution, and grain yield on Mollisols of Northeastern China, *Agronomy journal*, vol.110, no.4, pp.1607-1615.

[5] Guo M.J., Li J.Y., Li J., Qi J.R., Zhang X.Y., (2021), Changes of soil structure and function after 16-year conservation tillage in black soil, *Transactions of The Chinese Society of Agricultural Engineering*, vol.37, no.22, pp.108-118.

[6] He M., Gao H.W., Dong P.Y., Cui D.J., Zhao W.G., (2018), Sub-soiling experiment on double cropping and conservation tillage adopted area, *Transactions of the Chinese Society for Agricultural Machinery*, vol.49, no.7, pp.58-63.
[7] Issaka F., Zhang Z., Zhao Z.Q., Asenso E., Li J.H., Li Y.T., Wang J.J., (2019), Sustainable conservation tillage improves soil nutrients and reduces nitrogen and phosphorous losses in maize farmland in southern China, *Sustainability*, vol.11, no.8, pp.2397.
[8] Jia H.L., Jiang X.M., Yuan H.F., Zhuang J., Zhao J.L., Guo M.Z., (2017), Stalk cutting mechanism of no-tillage planter for wide/narrow row farming mode, *International Journal of Agricultural and Biological Engineering*, vol.10, no.2, pp.26-35.
[9] Jiang X.H., Tong J., Ma Y.H., Sun J.Y., (2020), Development and verification of a mathematical model for the specific resistance of a curved subsoiler, *Biosystems Engineering*, vol.190, pp.107-119.
[10] Mondal S., Chakraborty D., Das T.K., Shrivastava M., Mishra A.K., Bandyopadhyay K.K., Aggarwal P., Chaudhari S.K., (2019), Conservation agriculture had a strong impact on the sub-surface soil strength and root growth in wheat after a 7-year transition period, *Soil and Tillage Research*, vol.195, pp.104385-104385.
[11] Prathuang U., Kittikhun P., (2018), Performance of combined tillage tool operating under four different linkage configurations, *Soil and Tillage Research*, vol.183, pp.109-114.
[12] Qi H., Li C.F., Zhao M., Jiang Y., (2020), Developments and prospects of conservation tillage in the dryland of northern China, *Crops*, vol.36, no.2, pp.16-19.
[13] Qi J.Y., Wang X., Pu C., Ma S.T., Zhao X., Xue J.F., Zhang H.L., (2018), Research advances on effects of conservation tillage practice on soil nitrogen component, *Transactions of The Chinese Society of Agricultural Engineering*, vol.34, pp.222-229.
[14] Qu Y., Pan C.L., Guo H.P., (2021), Factors affecting the promotion of conservation tillage in black soil - The case of Northeast China, *Sustainability*, vol.13, no.17, pp.9563.
[15] Wang B., Xu J.G., Li W.H., (2021), Design and experiment on bionic vibrant subsoiler for corn fields in northern China, *Journal of Agricultural Mechanization Research*, vol.43, no.5, pp.104-108.
[16] Wang H.L., Zhang W., (2012), Optimization design on stubble-cutting disc with ripples of no-tillage planter, *Journal of Agricultural Mechanization Research*, vol.34, no.10, pp.102-105.
[17] Wang Q. Zhu L.T., Li M.W., Huang D.Y., Jia H.L., (2018), Conservation agriculture using coulters: Effects of crop residue on working performance, *Sustainability*, vol.10, no.11, pp.4099.
[18] Wang Z.Q., Wang W.X., Li X., Li W.C., Guo J.L., Tang M.J., Fang R., (2016), Development status of subsoiling at home and abroad under conservation tillage, *Journal of Agricultural Mechanization Research*, vol.38, no.6, pp.253-258.
[19] Zeng Z.W., Chen Y., (2018), The performance of a fluted coulter for vertical tillage as affected by working speed, *Soil and Tillage Research*, vol.175, pp.112-118.
[20] Zhang F.L., Ren Y.W., Lu C.J., Yu Y.F., Wu M.Q., Luo Y., Zhang Z.Y., Yang L., (2018), Effects of subsoiling on soil physical properties and crop yields, *Hubei Agricultural Sciences*, vol.57, pp.46-48.